Lung (2018) 196:165–171
https://doi.org/10.1007/s00408-018-0097-7

PULMONARY HYPERTENSION

Multiparametric Magnetic Resonance Imaging in the Assessment of Pulmonary Hypertension: Initial Experience of a One-Stop Study

Gisela M. B. Meyer[1] · Fernanda B. Spilimbergo[1] · Stephan Atmayer[2,3,6] · Gabriel S. Pacini[2,3,6] · Matheus Zanon[2,3,6] · Guilherme Watte[4,6] · Edson Marchiori[5] · Bruno Hochhegger[2,3,6]

Received: 31 October 2017 / Accepted: 5 February 2018 / Published online: 12 February 2018

Abstract

Introduction Our goal was to assess the diagnostic performance of magnetic resonance imaging (MRI) as a single method to diagnose pulmonary hypertension (PH) compared to right heart catheterization (RHC), computed tomography (CT), and ventilation/perfusion (V/Q) scintigraphy.

Methods We identified 35 patients diagnosed with PH by RHC in our institution who have also undergone a CT, a scintigraphy, and an MRI within a month. All cases were discussed in multidisciplinary meetings. We performed correlations between the MRI-derived hemodynamic parameters and those from RHC. The sensitivity and specificity of MRI were determined to identify its diagnostic performance to identify chronic thromboembolic pulmonary hypertension (CTEPH) and interstitial lung disease PH. The gold standard reference for the diagnosis of CTEPH and ILD was based on a review of multimodality imaging (V/Q scintigraphy and CT scan) and clinical findings.

Results Our results showed a good correlation between the hemodynamic parameters of cardiac MRI and RHC. Pulmonary vascular resistance had the best correlation between both methods ($r = 0.923$). The sensitivity and specificity of MRI to diagnose CTEPH was 100 and 96.8%, respectively. For the ILD-related PH, the MRI yielded a sensitivity of 60.0% and a specificity of 100%. Additionally, cardiac MRI was able to confirm all cases of PAH due to congenital heart disease initially detected by echocardiography.

Conclusions MRI represents a promising imaging modality as an initial, single-shot study, for patients with suspected PH with the advantages of being non-invasive and having no radiation exposure.

Keywords Pulmonary hypertension · Magnetic resonance imaging · Right heath catheterization · Computed tomography · Lung scintigraphy

✉ Gabriel S. Pacini
gabrielsartorip@gmail.com

[1] Pulmonary Hypertension Group, Santa Casa de Porto Alegre, Av. Independência, 75, Porto Alegre, Rio Grande Do Sul 90020-160, Brazil

[2] Federal University of Health Sciences of Porto Alegre, R. Sarmento Leite, 245, Porto Alegre, Rio Grande Do Sul 90050-170, Brazil

[3] Medical Imaging Research Laboratory, Federal University of Health Sciences of Porto Alegre, R. Sarmento Leite, 245, Porto Alegre, Rio Grande Do Sul 90050-170, Brazil

[4] Department of Respiratory Medicine and Thoracic Surgery, Irmandade da Santa Casa de Misericordia de Porto Alegre, R. Sarmento Leite, 245, Porto Alegre 90050-170, Brazil

[5] Federal University of Rio de Janeiro, Av. Carlos Chagas Filho, 373, Rio De Janeiro 21941-902, Brazil

[6] LABIMED – Medical Imaging Research Lab, Department of Radiology, Pavilhão Pereira Filho Hospital, Irmandade Santa Casa de Misericórdia de Porto Alegre, Av. Independência, 75, Porto Alegre 90020-160, Brazil

Introduction

Pulmonary hypertension (PH) is defined as a mean pulmonary artery pressure (mPAP) ≥ 25 mmHg at rest, measured by right heart catheterization (RHC) [1]. Normal mean mPAP at rest is around 14 ± 3 mmHg, with an upper limit of normality of 20 mmHg [2, 3]. Echocardiography is usually the initial imaging modality to screen for PH, but it might under or overestimate PAP and has limited value to differentiate most of the PH etiologies [4]. Computed tomography (CT) and ventilation/perfusion (V/Q) scintigraphy are important imaging modalities to identify the PH etiology, which defines treatment and prognosis [5, 6]. Also, cardiac magnetic resonance imaging (MRI) has become the gold standard method for the right ventricle (RV) assessment in patients with PH, as it has shown to be a valuable tool for monitoring treatment response and prognosis of these patients [5, 7, 8].

Although RHC is still the gold standard method to confirm PH and indicate the effectiveness of therapies in patients with PAH, it is an invasive procedure associated with several complications and even death at less experienced centers [3, 9]. Also, this method provides limited information about the etiology of PH and severity of heart remodeling [4]. Thus, there is an increasing interest in the use of MRI as a non-invasive method to estimate mPAP and also provide further information about the etiology of PH [4, 10]. Recent evidence has shown that cardiac MRI has greater accuracy than single-photon computed tomography (SPECT) to screen patients with chronic thromboembolic pulmonary hypertension (CTEPH) [11]. Also, recent technological advances have allowed MRI to be used in the diagnosis and monitoring of activity of Interstitial Lung Disease (ILD), although its accuracy is still lower than CT for this purpose [12].

Our goal was to study the diagnostic performance of cardiac MRI compared to CT and V/Q scintigraphy for the diagnosis of PH etiology. We further investigated the correlations between MRI and RHC in the assessment of hemodynamic and morphological parameters for PH.

Methods

Participants

We retrospectively identified 35 patients diagnosed with PH by RHC within 3 months of the echocardiography, between July 2013 and July 2016, who also underwent a CT, scintigraphy, and an MRI within a month. All cases were discussed in multidisciplinary meetings and the diagnoses were performed according to the current guidelines [1]. The median follow-up was 24 months. Patients were classified in functional class according to World Health Organization (WHO)/New York Heart Association (NYHA) [13]. Patients with connective tissue disease (CTD) were classified into group 3 (ILD-associated PH) either in the presence of evidence of extensive pulmonary disease (≥ 1/3 of lung fields involved) on high-resolution computed tomography (HRCT) or forced vital capacity of less than 60% of predicted [14, 15]. Treatment and prescription of therapies were in accordance with the current guidelines [1]. Informed consent was acquired from all patients at the time of the RHC. The local institutional board review approved the retrospective gathering of data.

Right Heart Catheterization

All exams were executed in the Catheterization Laboratory. RHC was performed through the right internal jugular vein with a 7-French Swan-Ganz catheter. The catheter was placed into the main pulmonary artery and hemodynamic parameters were calculated. Cardiac Output (CO) and cardiac index (CI) were estimated using Fick principle.

CT Protocol

All CT pulmonary examinations were performed with a 64-slice multidetector CT scanner (64-slice LightSpeed VCT scanner, GE Healthcare Technologies, USA). Images were obtained caudocranially, with breath hold at full inspiration. The following parameters were used: automated dose reduction 90–100 mA, 100–120 kV, 1.4 pitch, 0.5 s rotation time, 0.625 mm collimation, field of view (FOV) 400 × 400 mm. We administered 100 mL of intravenous contrast material (Iopromide, Ultravist 300; Bayer Schering, Germany) at 4–5 mL/s with bolus tracking used to trigger CT acquisition. High-resolution CT images were reconstructed for every 10 mm using a high spatial resolution filter.

MRI Protocol

MRI was performed using a 1.5T scanner (Magnetom AERA; Siemens, Germany). A half-Fourier single-shot turbo spin-echo sequence was used, and FOV was patient-adapted. The following sequence parameters were used: repetition time (TR)/echo time (TE)/flip angle, infinite/92 ms/150°; parallel acquisition factor, 2; slice thickness, 4 mm; distance factor, 20%; transversal (matrix, 380 × 256) and coronal (matrix, 400 × 320) orientations; and mean acquisition time of 90 s. A volumetric interpolated breath-hold examination (VIBE) sequence was chosen for fast T1-weighted MRI. Imaging parameters for the VIBE sequence were: TR/TE, 5.12/2.51 ms; flip angle, 10°; partition thickness, 4 mm with

no interslice gap; and matrix size, 256 × 116 with a three-dimensional breath-hold imaging technique. A T2-weighted fat-saturated BLADE (Siemens Medical Solutions) sequence was also used, with the following imaging parameters: TR/TE, 4670/113 ms; and partition thickness, 6 mm with no interslice gap.

The following measures were used for four-chamber and short-axis cine images: ECG-gated steady-state free-precession sequence, 20 frames per cardiac cycle, slice thickness 5 mm, FOV 48 × 43.2, matrix 256 × 256, BW 125 KHz/pixel, TR 3.7 ms, and TE 1.6 ms. The phase-contrast sequence was performed orthogonal to the pulmonary artery trunk with TR 5.6 ms, TE 2.7 ms, slice thickness 10 mm, FOV 48 × 28.8, and matrix 256 × 128. Regional lung perfusion was evaluated by means of three-dimensional delayed contrast enhancement (DCE) time-resolved angiography, with stochastic trajectories, or TWIST, using an eight-channel torso phased-array coil and the following MR imaging parameters: TR 2.1 ms, TE 0.7 ms, flip angle 25°; 40 three-dimensional datasets with an update rate of 1.0–1.2 s; matrix 192 × 113; FOV 50 × 42 cm; 0.04 mmol of gadoteric acid per kg (Dotarem®, Guerbet, Roissy CdG Cedex, France) delivered at 5 mL per second intravenously; and 30–36 reconstructed coronal sections (with a section thickness of 6 mm) covering the whole lung in a single breath hold.

Scintigraphy Protocol

A Krypton-81m generator was used for ventilation studies and Tc-99m Macro Aggregated Albumin (MAA-Tc99m) for perfusion studies. After injection of 11–185 MBq of MAA-Tc99m in the supine position, perfusion images were acquired simultaneously with ventilation images. A dual-head camera with a low-energy high-resolution collimator was used; at least 400,000 counts per image were acquired with a 256 × 256 pixel matrix.

Imaging Analysis

All CT and MRI images were reviewed by two chest radiologists (10 and 8 years of experience), blinded to RHC hemodynamics data. Disagreement between radiologists was solved by consensus; if consensus was not reached, a third radiologist with 15 years of experience made a final decision.

For the diagnosis of interstitial lung diseases on the CT, we considered the presence of usual interstitial pneumonia or non-specific interstitial pneumonia [16]. Obstruction of vessels, mosaic attenuation of pulmonary parenchyma, subpleural opacities, and chronic thromboembolic material within the pulmonary arteries were analyzed to exclude or diagnose CTEPH. The same tomographic criteria were applied for the diagnosis of pulmonary interstitial disease on the MRI. Perfusion MRI images were visually evaluated to determine whether perfusion was normal or reduced on a segment basis according to the literature [17].

A blinded chest radiologist (8 years of experience) processed the ventricular MRI segmentation and phase-contrast analysis with specialized software (CardiacVX, GE Healthcare, Waukesha, WI, USA), in accordance with the latest recommendations [18]. The contours of the main PA were traced simultaneously on magnitude and velocity-map images and peak velocity, PA blood flow, and PA distensibility were calculated [18, 19]. MRI-derived mPAP and PVR were estimated according to the regression model previously validated in a prospective cohort of patients with suspected PH [10].

Scintigraphic images were visually evaluated to determine whether perfusion was normal or reduced on a segment basis. Ventilation scintigraphic images were also assessed to determine whether ventilation was normal or reduced in each segment.

Statistical Analysis

Data were presented as mean ± SD or frequency and percentage. We performed associations between variables with χ^2 tests. For comparing continuous variables, a Student *t* test or an unequal variance *t* test was used. Pearson's or Spearman's rank correlation was used for assessment of the linear association between continuous variables. Coefficients were interpreted using the following parameters: 0.00–0.20 were considered very weak, ≥ 0.20–0.40 weak, ≥ 0.40–0.70 moderate, ≥ 0.70–0.90 strong, and ≥ 0.90 very strong [19]. The sensitivity and specificity of MRI to diagnose CTEPH and ILD were evaluated. The gold standard reference for the diagnosis of CTEPH and ILD was based on a review of multimodality imaging and clinical findings. In all cases, *P* values < 0.05 were considered to be statistically significant. All statistical analyses were performed using the SPSS v.18 (IBM, Chicago, IL).

Results

The characteristics of the study subjects are described in Table 1. The sample consisted of 35 patients, of which most were female ($n = 29$, 82.8%), had idiopathic PAH ($n = 18$, 51.4%), and were WHO functional class III or IV ($n = 19$, 54.2%).

Hemodynamic measurements from RHC and MRI are shown in Table 2. The correlation between MRI variables and invasively measured hemodynamics are shown in Table 3. The correlation between MRI-derived PVR demonstrated a very strong correlation to the PVR measured by the RHC ($r = 0.923$). The correlation of mPAP derived from

Table 1 Subjects' characteristics

Parameter	$N=35$
Female	29 (82.8)
Age (years)	41.7 ± 16.3
WHO/NYHA functional class	
Class I	6 (17.1)
Class II	10 (28.5)
Class III	14 (40.0)
Class IV	5 (14.2)
PH etiology	
Idiopathic PAH	18 (51.4)
Congenital heart diseases PAH	4 (11.4)
HIV-related PAH	2 (5.7)
Vasculitis PAH	1 (2.8)
Portopulmonary hypertension PAH	1 (2.8)
Connective tissue disease PH	5 (14.2)
CTEPH	4 (11.4)

Data are presented as mean ± SD or no. (%)

WHO/NYHA World Health Organization/New York Heart Association, *PH* pulmonary hypertension, *PAH* pulmonary arterial hypertension, *CTEPH* chronic thromboembolic pulmonary hypertension, *HIV* human immunodeficiency virus

Table 2 RHC and MRI hemodynamic parameters and imaging findings

RHC parameters	
Mean pulmonary artery pressure (mmHg)	48.7 ± 15.1
Pulmonary vascular resistance (wood)	7.8 ± 4.5
Cardiac output (L/min)	5.5 ± 1.9
Cardiac index (L/min/m^2)	3.3 ± 1.1
Right atrial pressure (mmHg)	7.6 ± 4.7
PCWP (mmHg)	8.9 ± 3.1
MRI	
Mean pulmonary artery pressure (mmHg)	40.6 ± 12.6
Pulmonary vascular resistance (wood)	8.7 ± 2.5
Ejection fraction (%)	47.4 ± 17.3
RV thickness (mm)	7.1 ± 4.4
Perfusion defects	5 (13.5)
Cardiac congenital abnormalities	4 (10.8)
Interstitial lung disease	3 (8.1)
Esophageal dilation	5 (13.5)
Liver cirrhosis	2 (2.7)

Data are presented as mean ± SD or no. (%)

PCWP pulmonary capillary wedge pressure, *MRI* magnetic resonance imaging, *RV* right ventricle

the two methods was also strong ($r=0.698$). Measurements of hemodynamic parameters stratified by NYHA functional class for both RHC and cardiac MRI are shown in Table 4. There was no statistical difference in the RHC-derived and MRI-estimated mPAP of the WHO groups I/II ($P=0.82$) and groups III/IV ($P=0.22$). The same finding was mirrored by the PVR estimated by both methods for WHO I/II ($P=0.59$) and WHO III/IV ($P=0.51$).

All five patients with CTD-related PH had evidence of extensive lung disease on HRCT and were qualified as group 3 (ILD PH), and MRI was able to detect ILD in three of them (Table 2) (sensitivity, 60%; specificity, 100%). Four patients were diagnosed with CTEPH in our cohort, and MRI could identify five patients with defects in pulmonary tree perfusion suggestive of CTEPH (sensitivity, 100%; specificity, 96.8%). The only false positive case is shown in Fig. 1. Additionally, cardiac MRI was able to detect all patients with PAH due to congenital heart disease (CHD) initially detected by echocardiography (sensitivity, 100%; specificity, 100%).

Discussion

Our study tested the diagnostic performance of MRI as a single non-invasive method to diagnose PH concerning both the hemodynamic parameters and the most likely etiology. We found a good correlation between MRI and RHC hemodynamic variables, which has already been validated in the literature [10]. Also, our study shows that MRI has a great accuracy to diagnose CTEPH and an acceptable performance to diagnose ILD compared to scintigraphy and CT, respectively. Furthermore, MRI-derived parameters of RV function such as RV mass, ejection fraction, and end-diastolic volume index have already been validated as prognostic markers and for monitoring of treatment response [18, 20].

Within our knowledge, this is the first work to study the feasibility of MRI as a single-imaging modality to provide the functional and etiological diagnosis of PH in comparison to RHC, HRCT, and scintigraphy for patients with ILD-related PH, CTEPH, and CHD. We presented a case that represents the challenges involved in the diagnosis of PH. In clinical practice, we rely on different imaging alternatives to investigate patients with suspected PH, and it is our duty to choose the most appropriate and less harmful modality to start with the investigation. Not infrequently patients undergo several imaging modalities associated with radiation exposure, such as CTs and scintigraphy, until a final diagnosis is provided. Thus, the application of MRI as an initial single-shot study is very tempting, since it has shown to diagnose PH by estimating mPAP and PVR [10], diagnose CTEPH with high accuracy, detect findings that may suggest ILD-associated PH, and identify congenital heart anomalies or LV dysfunction. This approach has the potential to reduce the use of invasive modalities, reduce exposure to radiation, and decrease costs (Table 5).

According to the current guidelines, RHC is the only method to directly measure mPAP and PVR and, therefore,

Table 3 Correlations between catheterization and MRI

Catheterization	MRI			
	Ejection fraction	RV thickness	Mean pulmonary artery pressure, (mmHg)	Pulmonary vascular resistance (wood)*
Mean pulmonary artery pressure, (mmHg)	0.033**	0.389**	0.698*	0.684*
Pulmonary vascular resistance, (wood)	−0.358**	0.407**	0.532*	0.923*
Cardiac Output (L/min)	0.494*	−0.095**	−0.132**	−0.634*
Cardiac index (L/min/m^2)	0.620*	−0.096**	−0.007**	−0.385**
Right atrial pressure (mmHg)	−0.325**	0.023**	−0.120**	0.098**
PCWP (mmHg)	0.136**	0.115**	0.057**	−0.161**

PCWP pulmonary capillary wedge pressure, *MRI* magnetic resonance imaging, *RV* right ventricle

*$P < 0.05$, **$P < 0.01$

Table 4 RHC and MRI hemodynamic parameters according to the functional class

Variable	Total	WHO functional class		Difference (*P*)
		I–II	III–IV	
RHC				
mPAP (mmHg)	48.67 ± 15.1	44.45 ± 13.4	53.95 ± 13.7	−9.50 (0.042)
PVR (woods)	7.82 ± 4.5	5.97 ± 2.5	9.70 ± 5.1	−3.73 (0.007)
CO (l/min)	5.52 ± 1.9	6.24 ± 2.1	4.96 ± 1.6	−1.28 (0.043)
CO index (l/min/m^2)	3.30 ± 1.1	3.65 ± 1.0	3.04 ± 1.1	−0.61 (0.098)
RAP (mmHg)	7.64 ± 4.7	5.93 ± 1.9	9.15 ± 5.8	−3.21 (0.030)
PCWP, mmHg	8.94 ± 3.1	8.93 ± 2.4	9.05 ± 3.6	−0.11 (0.912)
MRI				
mPAP (mmHg)	47.39 ± 17.3	45.47 ± 13.9	50.45 ± 19.0	−4.97 (0.141)
PVR (woods)	7.11 ± 4.4	5.51 ± 2.4	8.65 ± 5.0	−3.13 (0.021)
EF (%)	40.68 ± 12.7	46.35 ± 12.6	36.15 ± 11.3	−10.19 (0.014)
RV thickness (mm)	8.71 ± 2.5	8.06 ± 1.6	9.35 ± 3.0	−1.19 (0.036)

Data are presented as mean ± SD

RHC right heart catheterization, *MRI* magnetic resonance imaging, *mPAP* mean pulmonary arterial pressure, *PVR* pulmonary vascular resistance, *CO* cardiac output, *RAP* right arterial pressure, *PCWP* pulmonary capillary wedge pressure, *EF* ejection fraction, *RV* right ventricle

it becomes necessary for the follow-up of therapy response and progression of the disease [1]. However, due to a higher report of several complications, especially when realized in minor centers [9], the non-invasive methods have been extensively studied in the last decade to be used as alternatives for the patients' follow-up and assessment of therapeutic efficacy. Guo et al. [21] have shown that cardiac MRI is the best non-invasive method for monitoring of RV function and therefore the progression of the disease. The diagnostic performance of MRI to estimate RHC-derived mPAP and elevated PVR was shown to be very high [10]. Also, MRI parameters, such as PA distensibility, have great potential to screen patients who are likely to have a positive response in the RHC calcium-channel blocker test [22]. Thus, the applicability of RHC in a near future will become limited to exclude the diagnosis of PH by direct measurement of hemodynamic variables or confirm a finding suggested by the MRI.

In regard to the etiological investigation of PH, the V/Q scintigraphy remains as the initial screening test for patients with suspected CTEPH. However, computed tomography angiogram (CTA) may still be necessary to confirm the diagnosis and evaluate the extension of disease for surgical planning if considered [1]. Our study shows that MRI has a high accuracy to diagnose CTEPH, and previous authors have demonstrated that this modality can be even superior to radionuclide method [11]. Also, other advantages that favor the use of MRI as an initial test include avoiding exposure to ionizing radiation and no need for further confirmation with CTA to evaluate the pulmonary vascular characteristics. Dual-energy computed tomography (DECT) is a promising modality for the assessment of patients with PH, which has

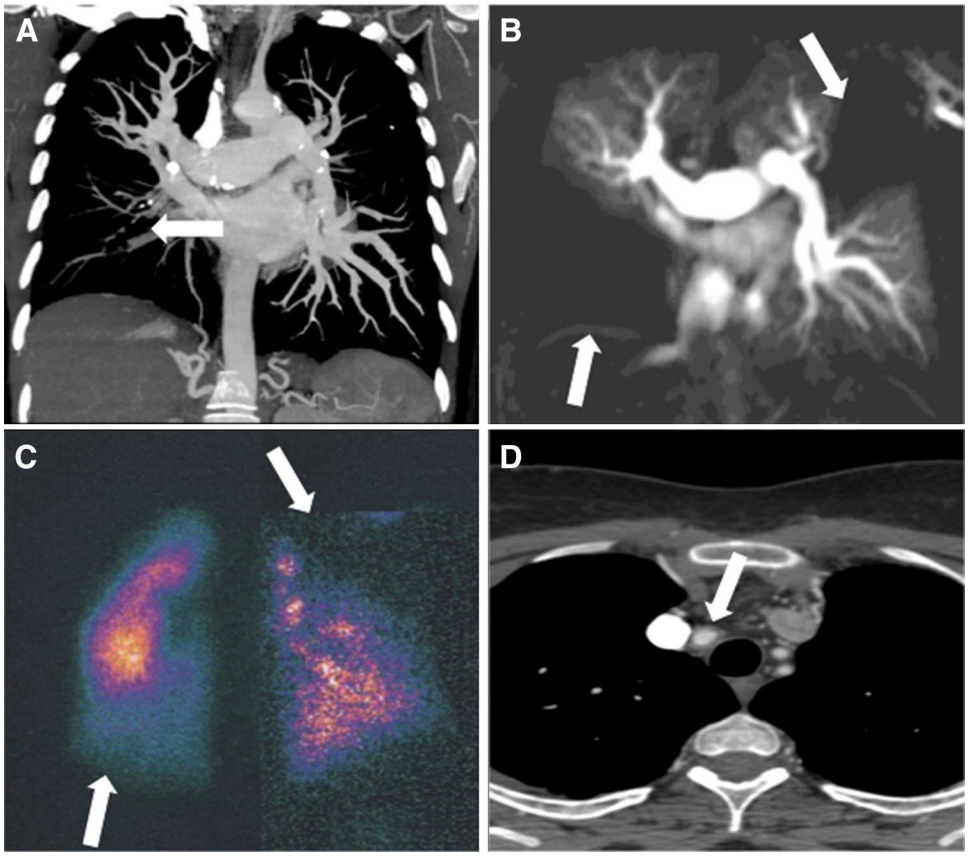

Fig. 1 Patient initially diagnosed with CTEPH suggested by all imaging methods. 46-year-old patient presented with long-standing dyspnea on exertion. **a** Computed angiotomography demonstrated filling defects and vascular amputation in the right lower lobe, compatible with chronic pulmonary thromboembolic disease. **b** Magnetic Resonance perfusion and **c** perfusion scintigraphy showed filling defects characteristic of chronic embolism. The initial diagnosis was chronic pulmonary thromboembolic disease. After 6 months of follow-up, the patient returned with pain in the right inferior limb. **d** Computed angiotomography showed arterial thickening of brachiocephalic trunk artery, compatible with Takayasu Arteritis (TA) and the patient was later confirmed to have pulmonary artery hypertension associated with TA

Table 5 Performance of MRI alone compared to the combination of CT, V/Q scintigraphy, echocardiography, and clinical data

Variable	Sensitivity (%)	Specificity (%)
CHD (group 1)	100	100
ILD (group 3)	60	100
CTEPH (group 4)	100	96.8

CHD congenital heart disease, *ILD* interstitial lung disease, CTEPH chronic thromboembolic pulmonary

shown higher accuracy than SPECT for CTEPH [23], with the advantage of evaluating the lung parenchyma. However, there are no data available to date comparing the accuracy of DECT and MRI for the diagnosis of CTEPH or other PH groups. Our study found that MRI has an acceptable accuracy for the diagnosis of ILD; however, HRCT is still superior for lung parenchyma assessment [12, 24, 25].

Despite the inherited benefits of non-invasive methods to the patient in comparison to invasive modalities, MRI has specific drawbacks that may limit their use in all patients. In regard to the specific limitations of ECG-gated and breath-hold imaging, acquisition of adequate images for patients with arrhythmias and those who cannot cooperate with breath holding is challenging and often implies an increased scanning time. Technological improvements such as self-gated imaging, non-breath hold, and real-time imaging are in the future to address these issues to obtain images with high temporal and spatial resolution for those patients [26–28].

Our study has some limitations. First, this is a preliminary study and has a small number of participants. Future studies with large samples are necessary to validate the results herein presented. Second, this is a retrospective study in which all participants already had a previous PH diagnosis. Thus, prospective studies are required to elucidate the potential of MRI to diagnose patients referred with suspected PH. Lastly, although the MRI has shown good accuracy for the diagnosis of elevated mPAP and identification of CHD, ILD, and CTEPH compared to other modalities, clinical and laboratory evaluation (e.g., family history, HIV testing) must be relied upon for most group 1 patients.

In conclusion, MRI has shown a promising potential to become an initial diagnostic test in patients with suspected PH. This method not only provides detailed information about hemodynamic and morphological parameters, such as mPAP, PVR, and RV function but is also applicable to provide the most likely etiology of PH.

Acknowledgements The authors thank Dr. Yuchi Han for her scientific contribution to improve this manuscript.

Compliance with Ethical Standards

Conflict of interest The authors declare that they have no conflict of interest.

Ethical Approval All procedures performed in studies involving human participants were in accordance with the ethical standards of the institutional and/or national research committee and with the 1964 Helsinki declaration and its later amendments or comparable ethical standards.

Informed consent Informed consent was obtained from all individual participants included in the study.

References

1. Galiè N, Humbert M, Vachiery JL et al (2016) 2015 ESC/ERS guidelines for the diagnosis and treatment of pulmonary hypertension. Eur Heart J 37:67–119
2. Kovacs MJ, Rodger M, Anderson DR et al (2003) Comparison of 10-mg and 5-mg Warfarin initiation nomograms together with low-molecular-weight heparin for outpatient treatment of acute venous thromboembolism: a randomized, double-blind, controlled trial. Ann Intern Med 138:714–719
3. Bane O, Shah SJ, Cuttica MJ et al (2015) A non-invasive assessment of cardiopulmonary hemodynamics with MRI in pulmonary hypertension. Magn Reson Imaging 33:1224–1235
4. Rajaram S, Swift AJ, Capener D et al (2012) Comparison of the diagnostic utility of cardiac magnetic resonance imaging, computed tomography, and echocardiography in assessment of suspected pulmonary arterial hypertension in patients with connective tissue disease. J Rheumatol 39:1265–1274
5. Grünig E, Peacock AJ (2015) Imaging the heart in pulmonary hypertension: an update. Eur Respir Rev 24:653–664
6. Swift AJ, Wild JM, Nagle SK et al (2014) Quantitative magnetic resonance imaging of pulmonary hypertension. J Thorac Imaging 29:68–79
7. D'Alonzo GE, Barst RJ, Ayres SM et al (1991) Survival in patients with primary pulmonary hypertension. Results from a national prospective registry. Ann Intern Med 115:343–349
8. Bradlow WM, Gibbs R, Mohiaddin JS RH (2012) Cardiovascular magnetic resonance in pulmonary hypertension. J Cardiovasc Magn Reson 14:6
9. Hoeper MM, Lee SH, Voswinckel R et al (2006) Complications of right heart catheterization procedures in patients with pulmonary hypertension in experienced centers. J Am Coll Cardiol 48:2546–2552
10. Swift AJ, Rajaram S, Hurdman J et al (2013) Noninvasive estimation of PA pressure, flow, and resistance with CMR imaging. JACC Cardiovasc Imaging 6:1036–1047
11. Johns CS, Swift AJ, Rajaram S et al (2017) Lung perfusion: MRI vs. SPECT for screening in suspected chronic thromboembolic pulmonary hypertension. J Magn Reson Imaging 46:1693–1697
12. Hochhegger B, Marchiori E, Irion K et al (2012) Magnetic resonance of the lung: a step forward in the study of lung disease. J Bras Pneumol 38:105–115
13. The Criteria Committee of the New York Heart Association (1994) Nomenclature and criteria for diagnosis of diseases of the heart and great vessels, 9th edn. Little, Brown & Co; Boston, pp 253–256
14. Condliffe R, Kiely DG, Peacock AJ et al (2009) Connective tissue disease-associated pulmonary arterial hypertension in the modern treatment era. Am J Respir Crit Care Med 179:151–157
15. Launay D (2007) Prevalence and characteristics of moderate to severe pulmonary hypertension in systemic sclerosis with and without interstitial lung disease. J Rheumatol 34:1005–1011
16. Travis WD, Costabel U, Hansell DM et al (2013) An official American Thoracic Society/European Respiratory Society statement: update of the international multidisciplinary classification of the idiopathic interstitial pneumonias. Am J Respir Crit Care Med 188:733–748
17. Hochhegger B, Ley-Zaporozhan J, Marchiori E et al (2011) Magnetic resonance imaging findings in acute pulmonary embolism. Br J Radiol 84:282–287
18. Swift AJ, Wild JM, Nagle SK et al (2014) Quantitative magnetic resonance imaging of pulmonary hypertension: a practical approach to the current state of the art. J Thorac Imaging 29:68–79
19. Hurdman J, Condliffe R, Elliot CA et al (2012) ASPIRE registry: assessing the spectrum of pulmonary hypertension identified at a referral centre. Eur Respir J 39:945–955
20. Peacock AJ, Vonk Noordegraaf A (2013) Cardiac magnetic resonance imaging in pulmonary arterial hypertension. Eur Respir Rev 22:526–534
21. Guo X, Liu M, Ma Z et al (2015) Assessing right ventricular function in patients with pulmonary hypertension based on noninvasive measurements: correlation between cardiac MRI, ultrasonic cardiogram, multidetector CT and right heart catheterization. J Cardiovasc Magn Reson 17:185
22. Jardim C, Rochitte CE, Humbert M et al (2007) Pulmonary artery distensibility in pulmonary arterial hypertension: an MRI pilot study. Eur Respir J 29:476–481
23. Ameli-Renani S, Rahman F, Nair A et al (2014) Dual-energy CT for imaging of pulmonary hypertension: challenges and opportunities. RadioGraphics 34:1769–1790
24. Kovacs G, Reiter G, Reiter U et al (2008) The emerging role of magnetic resonance imaging in the diagnosis and management of pulmonary hypertension. Respiration 76:458–470
25. McLure LE, Peacock AJ (2009) Cardiac magnetic resonance imaging for the assessment of the heart and pulmonary circulation in pulmonary hypertension. Eur Respir J 33:1454–1466
26. Contijoch F, Witschey WRT, Rogers K et al (2015) User-initialized active contour segmentation and golden-angle real-time cardiovascular magnetic resonance enable accurate assessment of LV function in patients with sinus rhythm and arrhythmias. J Cardiovasc Magn Reson 17:37
27. Contijoch F, Iyer SK, Pilla JJ et al (2017) Self-gated MRI of multiple beat morphologies in the presence of arrhythmias. Magn Reson Med 78:678–688
28. Usman M, Atkinson D, Odille F et al (2013) Motion corrected compressed sensing for free-breathing dynamic cardiac MRI. Magn Reson Med 70:504–516